ceramics

MDPI

Review

Synthesis of Bulk-Nucleated Glass–Ceramics and Porous Glass–Ceramic Composites through Utilization of Fly Ashes

Hugo R. Fernandes [1,*], Oguzhan Gunduz [2] and Dilshat U. Tulyaganov [3,*]

[1] Department of Materials and Ceramic Engineering, CICECO-Aveiro Institute of Materials, University of Aveiro, 3810-193 Aveiro, Portugal
[2] Centre for Nanotechnology & Biomaterials Research, Marmara University, Istanbul 34722, Turkey; oguzhan@marmara.edu.tr
[3] Department of Natural-Mathematical Sciences, Turin Polytechnic University in Tashkent, Tashkent 100095, Uzbekistan
* Correspondence: h.r.fernandes@ua.pt (H.R.F.); tulyaganovdilshat@gmail.com (D.U.T.)

Abstract: Coal combustion in power plants for electric power generation produces millions of tons of residues that are generally disposed of in landfills or ponds occupying vast land, resulting in serious environmental pollution. Fly ash (FA) is one of the main solid wastes generated in coal-based thermal power plants, representing the largest fraction of coal combustion residues (65–95%). Unfortunately, the enormous amount of FA residue is utilized only partly, mainly in the cement industry and building materials field. An alternative approach to using FA is its incorporation into ceramic, glass and glass–ceramic production, aligning with circular economy principles and reducing the environmental footprint of both the energy and ceramic sectors. In this review article, the topics of the composition, properties, classification, and utilization of fly ashes from thermal power plants are discussed. The main objective of this work is a critical analysis of the experimental trials directed to the involvement of FA as a raw material in the fabrication of glass–ceramics and porous ceramic composites.

Keywords: glass-ceramics; fly ashes; wastes; crystallization

check for updates

Citation: Fernandes, H.R.; Gunduz, O.; Tulyaganov, D.U. Synthesis of Bulk-Nucleated Glass–Ceramics and Porous Glass–Ceramic Composites through Utilization of Fly Ashes. *Ceramics* **2024**, *7*, 1014–1029. https://doi.org/10.3390/ceramics7030066

Academic Editor: Enrico Bernardo

Received: 19 June 2024
Revised: 19 July 2024
Accepted: 24 July 2024
Published: 30 July 2024

Copyright: © 2024 by the authors. Licensee MDPI, Basel, Switzerland. This article is an open access article distributed under the terms and conditions of the Creative Commons Attribution (CC BY) license (https://creativecommons.org/licenses/by/4.0/).

1. Introduction

Coal, being available in abundance, is a cheap fuel compared to other sources and a driving force for the energy generation needed to meet the global energy demand. The coal combustion in power plants for electric power generation produces millions of tons of residues. Residues produced by coal burning comprise boiler slag, bottom ash, fly ash, fluidized bed combustion ash, etc. [1]. Fly ash (FA) is the dust collected by dust extraction equipment, such as electrostatic precipitators or filter bags, from flue gas after coal combustion. FA is one of the main solid wastes generated in coal-based thermal power plants, representing the largest fraction of coal combustion residues (65–95%). For instance, a 1000 MW power plant uses around 12,000 tonnes of coal and generates around 2000 tonnes of fly ashes daily [2]. The disposal of these enormous amounts of FA is a major matter of concern because it represents a significant negative environmental impact including the leaching of potentially toxic substances into soils and groundwater, changes in the elemental composition of vegetation growing close to the ashes, and the accumulation of toxic elements in the food chain [3–5].

It is very difficult to handle FA in the dry state (mainly due to its fineness) because the flying fine particles of ash may corrode structural surfaces and negatively affect agriculture and the environment. It is also dangerous to the general population since long exposure to and inhalation of FA causes severe health problems like silicosis, fibrosis of the lungs, bronchitis, and pneumonitis [6].

Over the years, there has been an increasing interest in the use of FA for a variety of applications such as as a raw material or as an additive in the cement and concrete

industry, a raw materials substitute in the ceramic industry, soil stabilization for roads and embankments, landfill liners or covers, in mine filling, wastewater treatment, synthesis of glass–ceramics, zeolites, agriculture, etc. [7–9].

The main objective of this brief review is a critical analysis of the experimental trials directed to the involvement of FA as a raw material in the fabrication of glass–ceramics and foamed glass products. The discussion of the results is strictly confined to the physical, mechanical, and environmental properties of the bulk-nucleated glass–ceramics and porous glass–ceramic composites based on coal FA and their practical suitability.

2. Fly Ashes from Thermal Power Plants: Properties, Composition, and Classification

In the global scenario, more than 750 million tons of FA are produced annually worldwide [10]. The production and utilization of FA in the main world producers are depicted in Figure 1.

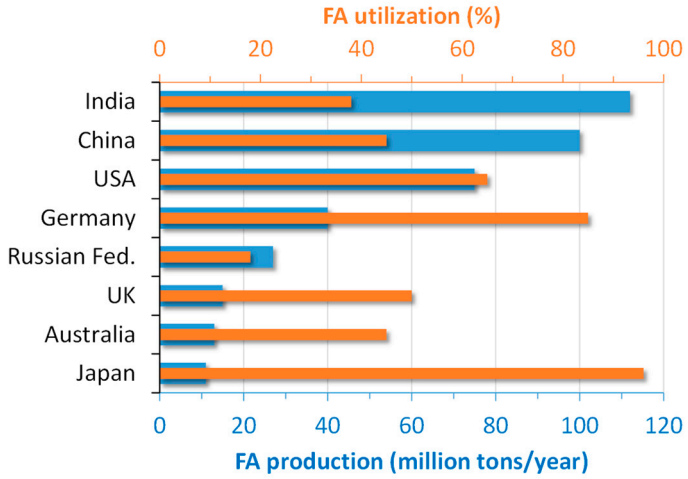


Figure 1. Production and utilization of FA in some countries (adapted with permission from [11], Elsevier 2019).

The physical, chemical, and mineralogical properties of FA are closely dependent on the nature of the used coal, the combustion conditions, the type of emission control device, and the storage and handling methods [12]. For instance, FA generated by the combustion of anthracite, bituminous, and lignite coal could present significant, different compositions and properties. The physical properties of fly ash vary widely depending on the coal type, boiler type, ash content in coal, combustion method, and collector setup [13].

FA is a solid powder at room temperature, occurring as fine particles with low to medium bulk density, high surface area, and light texture [12]. The appearance of FA is similar to cement, presenting a color ranging from light grey to grey black. The color of FA can reflect the amount of carbon content and, to a certain extent, the fineness of the FA: the darker the color, the finer the particle size of the FA and the higher the carbon content. For instance, the FA powders generated from anthracite and bituminous coal contain higher carbon residues, resulting in a dark brown color. On the other hand, FA powder from lignite and sub-bituminous coal contains less carbon residue and traces of calcium or lime show a grey color [14].

Regarding morphology, FA is a heterogeneous material containing powders of different shapes and sizes. Generally, it includes particles mostly spherical in size, along with rounded particles, although particles with angular and irregular shapes may also be present [14]. FA powder particles may be hollow (cenospheres) or filled with amorphous powder (plerospheres) [15]. The sizes of the spherical particles of FA may vary between 0.5 and 200 μm, while the other particles (with irregular and angular shapes) may be bigger in size [16]. For example, particle sizes of FA from bituminous and anthracite coals

are exceptionally similar to that of silt (<75 μm), whereas sub-bituminous and lignite FA particles are larger compared to other types (>75 μm) [11].

The bulk density of fly ash generated from different sources without any classification is quite different, most of which are between 1.9 and 2.9 $g \cdot cm^{-3}$. However, the bulk density among each particle may also vary due to their different compositions and structures, e.g., there are floating beads with a bulk density less than 1 $g \cdot cm^{-3}$ and iron beads with a bulk density greater than 3 $g \cdot cm^{-3}$ [17].

The composition of FA significantly depends on the coal type and technological processes used in thermal power plants. FA is usually produced at relatively high temperatures in the range of 1200–1700 °C and generated from various inorganic and organic constituents present in the used coals [18]. The most common elements presented in FA are O, Si, Al, Ca, Fe, C, K, Mg, H, Na, Ti, N, P, and Ba. Less common elements such as Mn, Sr, F, and Cl can also be present in FA [19].

FA is generally constituted by three different parts: (1) an inorganic, (2) organic, and (3) fluid constituent. The inorganic constituent is mainly composed of non-crystalline (amorphous, glassy particles) and crystalline (mineral) matter, such as crystals, grains, and aggregates of various minerals. The organic part comprises char materials and organic minerals, while the fluid constituent comprises liquid, gas and gas–liquid inclusions associated with both inorganic and organic matter [20]. Besides the glassy (amorphous) phase, the common phases present in FA include (in the order of decreasing amounts) mullite, quartz, char, hematite–magnetite, anhydrite–gypsum, feldspars, lime–portlandite, clay and mica minerals, cristobalite–tridymite, calcite–ankerite, corundum, jarosite, and some Ca and Ca–Mg silicates [19,21]. The chemical compositions of some types of FA produced in different counties are presented in Table 1.

Table 1. Summary of typical chemical composition (in wt.%) ranges of FA from some countries [16,22–24].

Country	SiO_2	Al_2O_3	Fe_2O_3	CaO	K_2O	MgO	SO_3	TiO_2	Na_2O	P_2O_5	LOI
Australia	31–69	17–33	1–27	0–5	0–3	0–2	0–0.6	1.2–3.7	0–1.5	0–4	na
China	36–57	19–55	2–19	1–7	0.8–0.9	0.7–5	1–3	0.2–0.7	0.6–1.3	1–1.5	nd
France	47–51	26–34	7–9	2–3	na	1.5–2	0.1–0.6	na	2–6	na	0.5–5
Germany	20–80	1–19	1–22	2–52	0–2	0.5–11	1–15	0.1–1	0–2	na	0–5
India	50–60	14–32	3–17	0.6–9	0.2–5	0.1–2	na	0.3–2.7	0.2–1.2	na	0.5–7
Japan	54–63	18–26	4–6	2–8	0.6–3	1–2	0.3–1.4	0.8–1.2	1.1–2.1	na	0.5–2
Russia	41–49	23–26	na	7–13	2–3	3–4	na	0.5–0.6	1.2–1.5	0.3–0.4	na
US	35–59	19–29	3–26	0.7–22	1–3	0.5–5	0.1–2	1–1.6	0.2–1.8	0.1–1.3	0.2–21

Note: na = not available; nd = not determined.

FA is generally classified into two chemical types for industrial application (mostly in concrete and cement production): Class F and Class C. The first type of FA comprises ≥70% of SiO_2 + Al_2O_3 + Fe_2O_3, whereas the second type has a sum of these oxides in the range of 50–70% [25]. The Class F type of fly ash is generated by the combustion of anthracite or bituminous coal, whereas Class C is generated by burning sub-bituminous coal or lignite. Class C fly ash usually exhibits cementitious properties along with siliceous and aluminous characteristics due to the presence of lime, whereas type F is rarely cementitious. Class C fly ash usually comes from coals which may generate ash with higher lime content generally, more than 15%, which in turn exhibits self-hardening characteristics due to the presence of more CaO. In other words, the availability of Class F is on a larger scale, and it generally has less lime, usually containing less than 15%, with a greater content of alumina, silica, and iron [26]. Other chemical requirements such as the ASTM classification of classes C and F include SO_3 content (which should be ≤5%), moisture (should be ≤3%), Na_2O (≤1.5%), particle size (34% ≤ 5% retained on 45 mm), and loss on ignition (LOI) (6–12% for Class F, considering performance).

However, FA can be classified according to different standards which are not universal, in terms of chemical composition (oxide content), chemical groups according to some

chemical and physical characteristics, loss of ignition (LOI), fineness, pH (acid and basic FA type), etc. [20]. Different methods are used by the European Union, Russia, and Canada to classify FA, and there is currently no international grouping system [27]. Table 2 presents a summary of some common classifications of FA.

Table 2. Summary of some common classifications of FA [20,22,25,28].

Criteria	Classification	Indicators
Chemical types	Class F	$\geq$70% SiO_2 + Al_2O_3 + Fe_2O_3
	Class C	50–70% SiO_2 + Al_2O_3 + Fe_2O_3
Chemical groups	Group I—silico-aluminate	$SiO_2/Al_2O_3 \geq 2$ and CaO < 15%
	Group II—alumino-silicate	$SiO_2/Al_2O_3 < 2$, CaO < 15%, SO_3 < 3%
	Group III—lime sulphate	CaO > 15% and SO_3 > 3%
	Group IV—basic FA	CaO > 15% and SO_3 < 3%
Particle size and specific surface area (SSA)	fine-grained	<25% are >75 µm, SSA > 3.0 $m^2 \cdot g^{-1}$
	medium-grained	0–75% are <75 µm, SSA 1.5–3.0 $m^2 \cdot g^{-1}$
	coarse-grained	<40% are <75 µm, SSA < 1.5 $m^2 \cdot g^{-1}$
Activity (content of free CaO)	inactive or very little active	<3.5% CaO
	slightly active	3.5–7% CaO
	active	7.0–14.0% CaO
	very active	>14% CaO
pH value	acidic	11–138–91.1–7.2
	low alkaline	11–138–91.1–7.2
	highly alkaline	11–138–91.1–7.2

3. Bulk-Nucleated Glass–Ceramic from Fly Ashes

FA is basically composed of silica, alumina, iron oxides, alkali and alkaline earth metal oxides plus several heavy metals and transition metal oxides, which are components commonly presented in the raw materials used in the ceramic and glass industry. By incorporating FA into ceramic and glass production, manufacturers can divert significant amounts of waste from landfills, aligning with circular economy principles and reducing the environmental footprint of both the energy and ceramic sectors. FA has also found application in the processing of glass–ceramic materials. Although the sintering process is steadily gaining more interest in the fabrication of glass ceramics from FA, in this article, the main attention is focused on glass–ceramic that is conventionally produced through devitrification of bulk glass by a single- or two-stage heat treatment [29–31].

Thus, the FA from Çayırhan Thermal Power Plant in Turkey was used as the principal precursor in glass fabrication with no additives and nucleating agents. As received, the FA sample had a chemical composition (in wt.%) of 42.82 SiO_2, 16.38 CaO, 5.85 MgO, 7.01 Fe_2O_3, 13.36 Al_2O_3, 5.06 Na_2O, 1.83 K_2O, and 6.47 SO_3 and comprised crystalline phases, namely quartz, mullite, enstatite, anorthite, and hematite. The fly ash sample was melted in Pt-crucibles at 1400 °C for 4 h, and then the melt was poured into the water; glass frit, after drying, was crushed, pulverized, and remelted at the same temperature for 10 h, followed by casting in a preheated, graphite mold. To fabricate the as-cast glass–ceramic, the glass was heat-treated at 680 °C for 5, 10, and 15 h for nucleation and then at 924 °C for 20 min for crystal growth. The diopside-based glass–ceramic sample nucleated at 680 °C for 5 h demonstrated the highest microhardness value of 907 $kg.mm^{-2}$ (8.89 GPa) [32].

Vitrification of a glass batch composed of merely coal FA was found to be difficult, and crystallization of the molten glass was not possible without modifying the composition of the FA through the addition of selected oxides [33]. Ark shell (as a source of calcium) and TiO_2 (as a nucleating agent) were added to the glass batch in order to decrease the melting temperature and promote internal crystallization. The iron and titanium oxides present in the ash components and added materials have a combined effect on the nucleation. The glass devitrified through a single-stage heat treatment, during a non-isothermal process:

melting proceeded in Pt-Rh crucibles at 1450 °C for 3 h, and then the melt was poured into a graphite mold preheated to 750 °C. Crystallization via nucleation and crystal growth is processed as a simple cycle heating process at 950–1050 °C for 10–240 min. The glass–ceramics produced demonstrated a density of 2.77–2.81 $g \cdot cm^{-3}$, a bending strength of 98–176 MPa, a fracture toughness of 1.12–3.10 $MPa \cdot m^{1/2}$, an elastic modulus of 91–100 GPa, and a CTE of (5.5–6.5) $\times 10^{-6}$ K^{-1}. Generally, with a temperature and holding time rise, the aspect ratio of the crystal increased, leading to a higher mechanical strength of resulting glass–ceramics. Importantly, the effect of temperature on the crystal growth was more pronounced than that of holding time. It was found that at 1050 °C, only a short time was needed to obtain glass–ceramics with a high strength, while at a temperature above 1050 °C the material deformed after 30 min due to approaching a low-viscosity region.

The experimental results demonstrated that an appropriate ratio between the glass network former and modifiers is crucial to obtain suitable glass and glass–ceramic products. Consequently, glasses and glass–ceramics were produced by incorporating up to 50 wt.% of Italian or Spanish coal fly ash with glass cullet and float dolomite. The batch was melted at approximately 1500 °C (with thermal cycles of 5 h), after which the glass was poured into a steel mold, annealed at 550 °C for 2 h, and heat-treated in the interval 900–1200 °C for 0.5–8.0 h [34]. In all the investigated fly ash glass compositions, no induction time of nucleation and crystallization was detected since the crystal growth rate was very fast, occurring from very short thermal treatment times. The mechanical properties of the glass–ceramic products were as follows: fracture toughness 0.70–3.00 $MPa \cdot m^{1/2}$ (KIC), elastic modulus 42–92 GPa (E), and microhardness 4.6–7.3 GPa (HV). The experimental glass 4T had a composition in wt.% of 50.07 SiO_2, 17.00 CaO, 8.7 MgO, 3.62 Fe_2O_3, 14.71 Al_2O_3, 4.39 Na_2O, 0.69 K_2O, and 0.82 TiO_2 after heat treatment at 1200 °C, devitrified to feldspar, pyroxene, and spinel phases, and demonstrated high KIC, E, and HV values.

The possibility of the effective utilization of FA originating from a coal-burning thermal power plant was investigated as one of the starting materials to synthesize wollastonite-based glass ceramics [35]. FA supplied from a Rayong (Thailand) coal-burning thermal power plant had the following chemical composition, in wt.%: 41.62 SiO_2, 23.11 Al_2O_3, 14.92 CaO, 1.59 MgO, 6.03 Fe_2O_3, 1.15 Na_2O, and 1.59 K_2O. The raw FA comprised some quantity of glassy phase and crystalline phases, α-Quartz (SiO_2), anorthite ($CaAl_2Si_2O_8$), gehlenite ($Ca_2Al_2SiO_7$), and the percent crystallinity was evaluated to be around 2%. CaF_2 was added as a nucleating agent and spodumene [$LiAl(SiO_3)_2$] was also added for a reduction in the thermal expansion coefficient. Glass was prepared by mixing and melting the batch containing 35% of fly ash in a Pt/Rh10 crucible using an electric furnace at 1450 °C for 2 h. The melt was poured onto an iron plate, and then crushed and remelted under the same conditions. This refined melt was again poured onto an iron plate. Bubble-free and dark green glass was obtained. The samples were then annealed at just above the T_g for 30 min and cooled to room temperature in the furnace. They were then heat-treated for nucleation and crystallization under various conditions. Crystallization exothermic peaks appeared at 970 °C for G0 (zero CaF_2) glass and 900 °C for G3 (3% CaF_2) and G5 (3% CaF_2 and 20% spodumene) glasses. It was clear that the addition of CaF_2 and spodumene reduced the crystallization temperature. Experimental glasses were heat-treated at 750 °C for 10 h and further at 950 °C for 5 h for crystal growth. Surface crystallization was revealed for G0 glass while CaF_2-containing glasses G3 and G5 exhibited bulk crystallization resulting in the highest values of bending strength of 206 and 230 MPa, respectively [35].

A preliminary study of the co-utilization of wastes, namely ferronickel slag FNS (65–80 wt.%) and coal fly ash FA (20–35 wt.%), for preparing glass–ceramics revealed that the suitable glass contained 75 wt.% FNS and 25 wt.% FA and its chemical composition was as follows, in wt.%: 49.55 SiO_2, 21.36 CaO, 3.76 MgO, 9.39 FeO, and 10.15 Al_2O_3. By controlling the crystallization of the melted mixture at 867 °C for 2 h, an enstatite–spinel-based glass–ceramic was obtained featuring a density of 3.11 $g \cdot cm^{-3}$, a bending strength of 116 MPa, an acid resistance of 99.97%, and an alkali resistance of 99.70% [36].

As a continuation of the previous work [36], the effect of Cr_2O_3 content (varied from 0 to 2.0 wt.%) on the crystallization of glass containing 75 wt.% FNS and 25 wt.% FA was studied [37]. The flow chart of the preparation of glass–ceramics from coal fly ash (CFA) and ferronickel slag (FNS) that are typical for preparation of bulk glass–ceramic is shown in Figure 2. The raw materials were mixed and then melted at 1550 °C for 1 h to obtain homogeneous glass. The as-cast glass was annealed at 650 °C for 2 h followed by heat treatment in non-isothermal conditions with a heating rate of 10 K·min^{-1} to produce glass–ceramics.

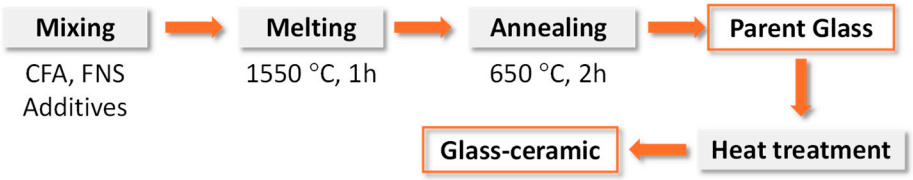


Figure 2. Flow chart of preparation of glass–ceramics from coal fly ash (CFA) and ferronickel slag (NS) (adapted with permission from [37], Elsevier 2023).

Crystallization kinetics studies demonstrated that with the rise in Cr_2O_3 content from 0 (Cr0) to 1.6 (Cr1.6) wt.%, the crystallization mode of the parent glass changed from surface crystallization to bulk crystallization whilst the activation energy decreased from 448.23 to 232.65 kJ. mol^{-1}. With a further Cr_2O_3 content increment to 2.0 (Cr2.0) wt.%, the activation energy for crystallization increased to 304.21 kJ. mol^{-1} and the crystallization mode went back to surface crystallization. The properties of synthesized bulk glass–ceramics are demonstrated in Figures 3 and 4. An optimal content of Cr_2O_3 was established to be 1.6 wt.%, which caused the formation of a dense glass–ceramic having a main crystalline phase of enstatite and a secondary crystalline phase of spinel. This glass–ceramic material featured a density of 3.17 g·cm^{-3}, a bending strength of 175 MPa, a Vickers microhardness of 9.51 GPa, an acid resistance of 99.99%, and an alkali resistance of 99.97%.

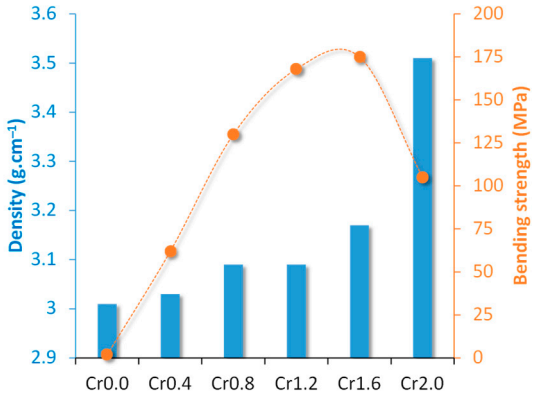


Figure 3. Densities and bending strengths of Cr0-Cr2.0 bulk-nucleated glass–ceramics (adapted with permission from [37], Elsevier 2023).

It was well documented elsewhere [38–40] that Cr_2O_3 significantly increases the crystallization rate only for Fe-containing compositions as the corresponding mechanism includes the formation of spinels, which, in turn, actively catalyze the formation of pyroxene phases. The first step of the heat treatment, at a lower temperature, is connected with the formation of heterogeneous nuclei, i.e., small crystallites promoting the growth of the major crystal phase. The higher the number of nuclei formed, the finer the structure of the glass–ceramics and the better the properties of the material.

Cr_2O_3, as a nucleating agent, was used to produce mono-mineral augite-type GCs from low-silica and high-calcium fly ash [41–44]. This FA derives from the burning of lignite in the thermal power stations of Ptolemaida (Northern, Greece). Lignite plays an important

role in Greece's energy sector as it satisfies over 67% of the country's needs in electric power. Lignite deposits are located in three regions of Greece, namely Ptolemais–Amynteo, Florina, and Megalopolis, where the annual production of lignite is around 60 million tons, while each year, approximately 10 million tons of lignite fly ash is produced in Greece [45]. FA from the thermal power stations of Ptolemaida was used as the principal raw material in glass–ceramic fabrication. Its average chemical composition in wt.% was 30.03 SiO_2, 13.67 Al_2O_3, 38.87 CaO, 5.32 Fe_2O_3, 4.42 MO, 0.63 Na_2O, 0.59 K_2O, 6.17 SO_3, and 0.30 TiO_2; the XRD spectra and an SEM image of FA are shown in Figure 5.

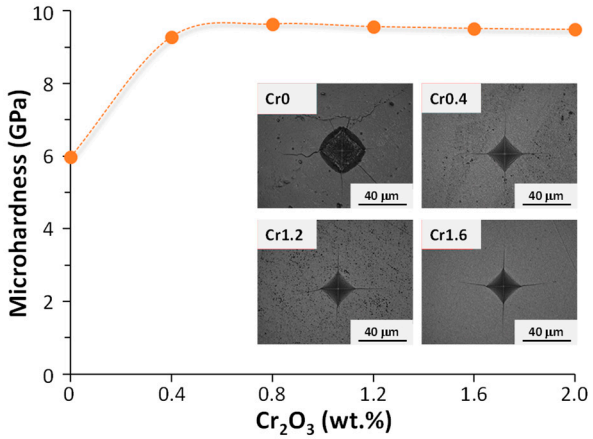


Figure 4. Vickers microhardness of Cr0-Cr2.0 bulk-nucleated glass–ceramics (adapted with permission from [37], Elsevier 2023).

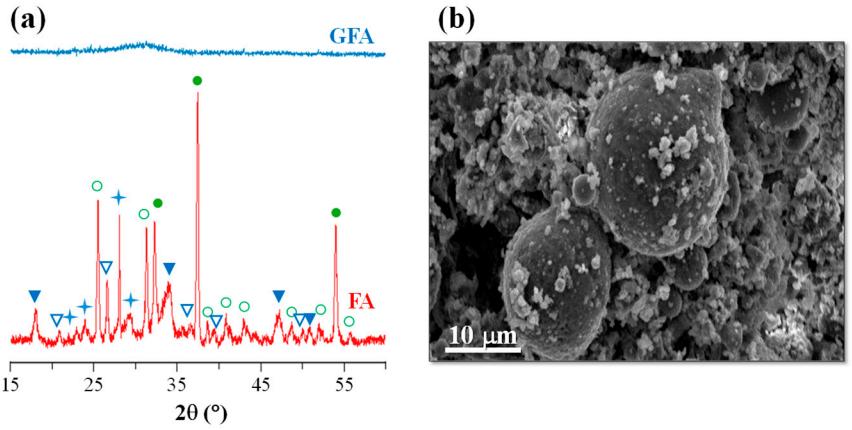


Figure 5. (**a**) XRD spectra of as-received FA (● calcium oxide (CaO); ○ anhydrite ($CaSO_4$); ▽ quartz SiO_2; ▼ portlandite $Ca(OH)_2$; ✦ calcium aluminum silicate) and (**b**) SEM image of as-received FA (adapted from [42], SAGE Publications, 2009).

A parent glass (C1) with nominal composition intended to be close to $CaMg_{0.75}Al_{0.4}Fe_{0.1}Si_{1.75}O_6$ was produced with silica, alumina, and magnesium carbonate added to the batch; Cr_2O_3 was introduced in the amounts of 0.50 wt.%, 0.75 wt.%, and 1.0 wt.% (over 100% of nominal composition) which resulted in the compositions C2, C3, and C4, respectively. Homogeneous mixtures of the batches were melted in alumina crucibles at 1500–1550 °C for 1 h and glasses in bulk form were produced by casting of the molten glass on preheated (500 °C) bronze molds. The T_g of the glasses ranged between 665 °C and 690 °C and the T_s between 761 °C and 778 °C. All investigated compositions featured a single exothermic crystallization peak (T_p) between 900 °C and 1000 °C (Figure 6a)—this peak is shallow and occurs at a high temperature in the case of C1 but it is much sharper and occurs at lower temperatures in C2 and more pronouncedly in C3 and C4. The effect of the Cr_2O_3 on nucleation (promoted by heat treatment close to the T_g, ~700 °C, for 1 h) and

crystallization (promoted by heat treatment in the range of the T_p for 2 h) was evaluated by the difference in density between the parent glasses and the GCs (Table 3), which reflects the degree of conversion and the formation of crystalline phases (e.g., for the same temperature of heat treatment, C3 and C4 feature the highest degree of crystallization). Basically, the density of Cr_2O_3-nucleated C2, C3 and C4 compositions was not significantly influenced by heat treatment temperature rise (Table 3).

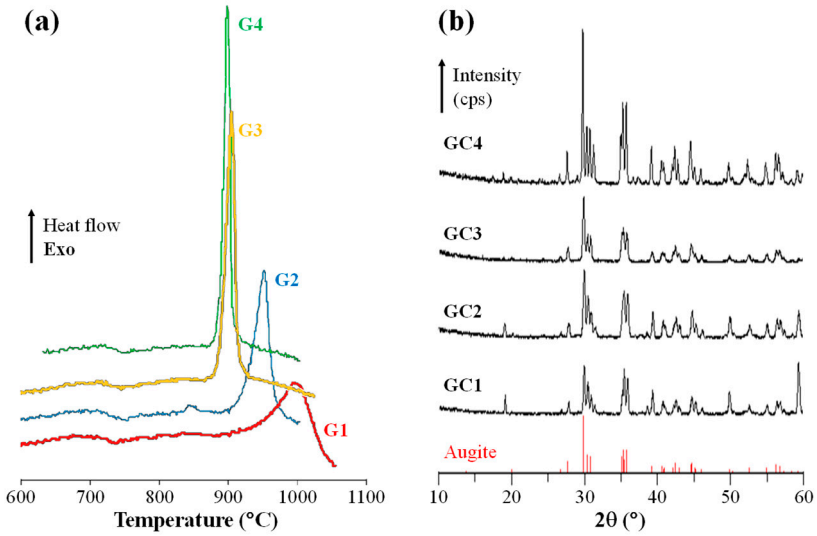


Figure 6. (**a**) DTA plots of fine powders (glass frit) of the four investigated glasses and (**b**) X-ray diffractograms the GCs crystallized at 900 °C for 2 h (adapted from [42], SAGE Publications, 2009).

Table 3. Density of the parent glasses and glass–ceramics crystallized at different temperatures for 2 h (standard deviations < 0.01 g·cm^{-3}) [37].

Content of Cr_2O_3 (wt.%)	Density (g·cm^{-3})			
	Initial Glass	2 h at 900 °C	2 h at 950 °C	2 h at 1000 °C
0	2.91	2.93	2.93	2.96
0.5	2.91	3.05	3.04	3.04
0.75	2.92	3.11	3.08	3.08
1.00	2.93	3.10	3.11	3.10

The heat treatment at 900 °C predominantly results in a single crystalline phase of augite (Ca, Mg, Fe, Na)(Mg, Fe, Al, Ti)(Al, Si)$_2O_6$, which belongs to the family of pyroxenes (Figure 6b). Increasing the Cr_2O_3 content causes an improvement in crystallinity, which is evidenced by the increasing intensity and sharpening of the diffraction peaks.

Figure 7 illustrates the impact of Cr_2O_3 on the microstructure of the glass–ceramics. The Cr_2O_3-free GC C1, crystallized at 1000 °C (Figure 7a), presents a structure with coarse crystal layers embedded in a highly chemical-resistant glassy phase. Observations at the sample edges confirmed that crystallization initiates from the surface.

The presence of Cr_2O_3 led to fine-grained bulk-crystallized GCs after heat treatment at a relative low temperature (900 °C), which is consistent with DTA results. The microstructure of GC C3 (0.75% Cr_2O_3) crystallized at 900 °C (Figure 7b) shows submicron crystals perfectly bordered one to the other. Observations of the bulk and surface of GCs C2 and C3 revealed no surface crystallization, which confirms that the Cr_2O_3-free C1 glass tends to surface crystallization, whereas the presence of Cr_2O_3 promotes bulk crystallization, as seen in GCs C2, C3, and C4.

GC C3 crystallized at 900 °C, demonstrating a high flexural strength that was ~200 MPa. The CTE values of the GCs C2, C3, and C4 crystallized at 900 °C, determined by the slope of dilatometry curves, were 8.81 × 10^{-6} K^{-1}, 9.55 × 10^{-6} K^{-1}, and 9.36 × 10^{-6} K^{-1}, respectively. The calculated electrical resistivity for GC 3 was 1.40 × 10^6 Ω·cm and for GC4 it was

5.78×10^5 Ω·cm (at 1000 °C), which are comparable with the data obtained from conventional electrical insulators made from alumina (7×10^6 Ω·cm) [46] and cordierite–anorthite composites (4.6×10^5 Ω·cm) [47] at 1000 °C. Bulk and porous GCs were produced through bulk nucleation and controlled crystal growth of parent glass manufactured from the fly ash of St. Dimitrios Power Plant, situated in Western Macedonia, Greece [48]. Ash samples, following dehumidification at 170 °C for 1 h, were stratified by sieving to obtain grain sizes below 65 μm. The glass batch comprising fly ash (30 wt%) and glass cullet (70 wt%) was melted in alumina crucibles at 1400–1500 °C for 0.5 h, but was first heat-treated at 1200 °C, ensuring the embodiment of the fly ash particles within the melt and aiming for proper homogenization. The bulk glasses were produced by casting the molten glass in preheated (500 °C) bronze molds and annealing them at 700 °C for 1h in order to release residual stresses. Nucleation and crystallization were conducted at a rate of 1.5 K·min^{-1} in the interval of 900–1050 °C (with 50 °C intervals) for 1.5 h. Mechanical testing revealed the influence of the heating strategy on the products' strength characteristics. Thus, glass samples subjected to heat treatment at 1050 °C exhibited a 21% increment in bending strength (~205 MPa) compared to those treated at 900 °C. This was attributed to the formation of a finer microstructure, confirmed by SEM investigation. The differences in strength observed for the samples produced at the two different melting temperatures of 1400 °C and 1500 °C were found to be statistically insignificant.

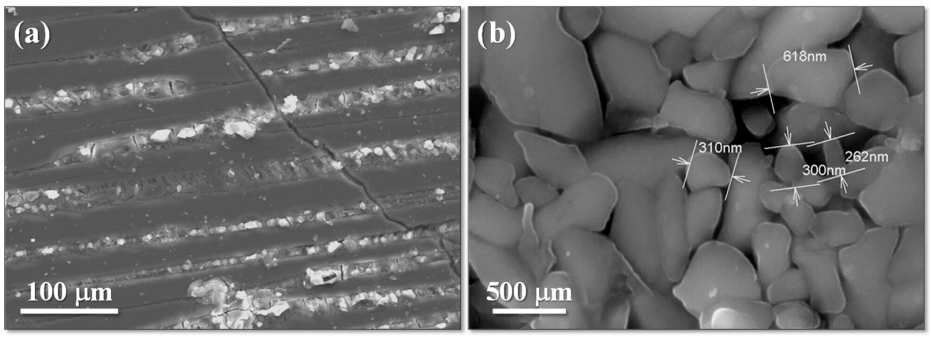


Figure 7. Microstructures of (**a**) the Cr_2O_3-free glass–ceramic C1 crystallized at 1000 °C, and (**b**) the 0.75% Cr_2O_3-containing glass–ceramic C3 crystallized at 900 °C (adapted from [42], SAGE Publications, 2009).

Elsewhere [49], a systematic evaluation of the sustainability of recycling fly ash, from thermal power plants, into novel glass–ceramics (GCs) was provided and concluded that using fly ash as substitute of conventional materials during the production of high-added-value products has a significant environmental potential, next to the obvious benefit of raw material saving. Table 4 provides a comparison of the properties of some bulk-nucleated GCs produced from different fly ashes [50,51].

Table 4. Properties of the presented bulk-nucleated GCs produced from different fly ashes.

Ref.	Nucleating Agent (%)	Micro-Hardness (GPa)	Flexural Strength (MPa)	CTE ($\times 10^{-6}$ K^{-1})	Density (g·cm^{-3})	Fracture Toughness (MPa·m$^{1/2}$)
[32]	Not added	8.89	n/r	n/r	n/r	n/r
[33]	2–11 TiO_2	6.20–7.60	98–176	5.5–6.5	2.77–2.81	1.12–3.10
[34]	Not added	4.6–7.3	n/r	n/r	n/r	0.70–3.00
[35]	3 CaF_2	n/r	135–230	8.5–9.0	2.66–2.72	n/r
[36]	Not added	n/r	116	n/r	3.11	n/r
[37]	0.4–2.0 Cr_2O_3	9.28–9.63	62–175	n/r	3.03–3.51	n/r
[41,42]	0.5–1.0 Cr_2O_3	n/r	200	8.8–9.5	3.04–3.11	n/r

"n/r" stands for "not reported".

4. Porous Glass–Ceramic Composites from Fly Ashes

FA is a cheap and abundant product, rich in minerals containing silicon and aluminum, making it suitable as a starting material for foamed ceramics. Foamed ceramics have the advantages of high porosity, large specific surface area, high strength, and high temperature resistance. They are widely used in industrial sewage treatment, automobile exhaust equipment, heat and sound insulation material, and the filtration of molten metal extending to the field of aviation, electronics, and biochemicals [52–56].

The utilization of FA to produce foam glass and glass–ceramic composites not only provides a valuable way to recycle industrial waste but also offers economic and environmental benefits. It reduces the need for natural raw materials like kaolin or bauxite, quartz, [52,53] and silica micro powder, which are typically used in foamed-ceramic production, thus conserving natural resources while mitigating the environmental impact associated with fly ash disposal, such as landfilling.

Foam glass and glass–ceramic foam are porous, heat-insulating, and soundproof materials, with a true porosity up to 90 vol.%. Generally, they are produced by the powder method when a mixture of glass powders and special additives facilitating the formation of a gaseous phase is sintered upon heating. These additives introduced into a glass foam batch in small quantities are called pore-forming or gas-forming agents. Under thermal treatment of such a mixture, when the temperature exceeds the softening temperature glass particles start sintering and form a continuous sintered body. Particles of the pore-forming agent become insulated by the softened glass. After a certain temperature is reached, they start emitting gases, frothing the glass melt. Due to gas emission, pores emerge in all parts of the sintered body where the particles of the pore-forming agent have been blocked. The shape of pores and the properties of foam glass obtained largely depend on the concentration and type of the foaming agent used. In its physical aspect, foam glass is a heterogeneous system consisting of gaseous and the solid phases. The solid phase is amorphous or devitrified glass that forms thin walls of single cells several micrometers thick. The cells are filled with the gaseous phase.

Nowadays, extensive research has been conducted to produce glass–ceramic foams using metallurgical slag, municipal solid waste, waste glass and fly ash, polishing porcelain stoneware tile residue, etc. [2,53–64]. Likewise, new technologies, such as replica, sacrificial template, and direct foaming methods, have been developed. Direct foaming is the simplest and most common method, involving the sintering of raw materials with a small amount of additives [53,56,60]. These additives, known as pore-foaming agents, create porosity by releasing gas that froths the glass ceramic melt at relatively high temperatures. The concentration and type of pore-foaming agent can significantly affect the pore size and structure of the resulting glass ceramic foams.

Porous glass–ceramic composites based on waste silicomanganese slag (SMS) and fly ash (FA) as raw materials and silicon carbide (SiC) as a foaming agent were systematically investigated [56]. Figure 8 presents a schematic illustration of the foamed-glass–ceramic preparation process. The mixture of FA and SMS was thoroughly blended with a specific quantity of water, pressed, dried, and then sintered in a furnace at 1050–1170 °C for 45 min at a heating rate of 5 K·min^{-1}. Figure 9 presents the cross-sectional morphology of the specimens sintered at various temperatures, evidencing the increasing of the size and number of pores with the rising of the temperature [53]. The best overall performance was achieved for compositions comprising 20 wt.% SMS and 80 wt.% FA as raw materials, with a SiC addition of 1.0 wt.% and a sintering temperature of 1100 °C (Figure 9), compressive strength, bulk density, and total porosity of 8.09 MPa, 0.57 g·cm^{-3}, and 71.04%, respectively. These properties make it suitable for application as an insulating material or as a decorative material for building partitions [53].



Figure 8. Schematic illustration of the foamed glass–ceramic preparation process (adapted from [53], MDPI, 2023).

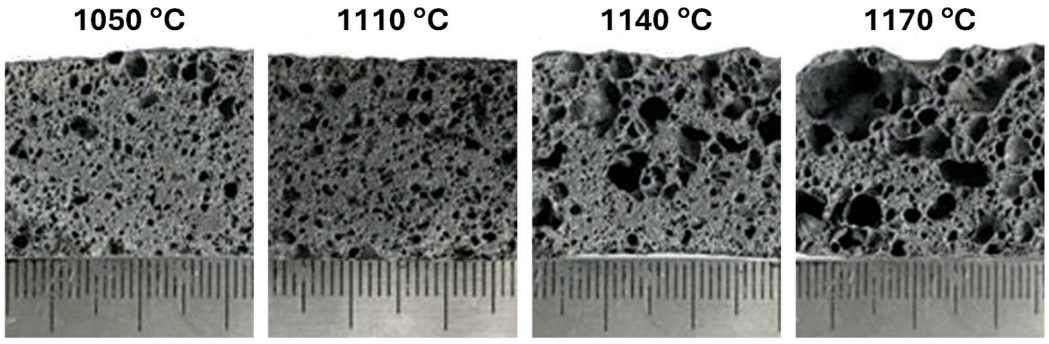


Figure 9. The cross-section macrostructure of the samples at different temperatures (adapted from [53], MDPI, 2023).

Glass–ceramic composites were prepared by the direct foaming method using coal fly ash (FA) and waste glass as primary materials, with borax and calcium carbonate serving as fluxing and foaming agents, respectively [60]. The study systematically investigated the effects of coal FA additions, foaming time, heating rate, and sintering temperature on bulk density, porosity, mechanical properties, and thermal conductivity. The bulk density and compressive strength of porous ceramics increase with the increasing of sintering temperature, while the apparent porosity and water absorption decrease. The experimental results indicated that the optimal parameters for fabricating glass–ceramic foams were achieved after sintering at 800 °C for 45 min, using 40 wt.% coal FA, 60 wt.% waste glass, 30 wt.% borax, and 0.5 wt.% calcium carbonate. The obtained foams exhibited a low bulk density of 0.46 g·cm^{-3}, a compressive strength exceeding 5 MPa, and a low thermal conductivity ~0.36 W·m^{-1}K^{-1} [60].

Glass–ceramic composites were synthesized utilizing cullet from sheet glass and FA derived from thermal power stations, incorporating carbonates such as commercial dolomite and calcite-based sludges to act as foaming agents [2]. The study assessed how the type and content of foaming agents, along with the sintering temperature, affected the resulting foam glass's apparent density, compressive strength, microstructure, and crystalline phase composition. To achieve the objective of integrating a suitable quantity of FA, five distinct carbonate-free mixtures were formulated consisting solely of glass and FA in varying proportions of glass cullet (G) and fly ash (A), i.e., G/A: G90A10, G80A20, G70A30, G60A40, and G50A50. The preparation process involved dry mixing the components in a cylindrical rotary mixer for 30 min. Cylindrical pellets measuring 20 mm in diameter and 3 mm in thickness were produced through uniaxial pressing at 80 MPa and sintered at temperatures of 800 and 900 °C for 20 min. Subsequent evaluations included measuring the apparent densities and shrinkage and visual ex-amination of the samples to achieve the highest feasible ash integration into the mixture and the capability to create porous structures; a composition comprising 80 wt.% glass and 20 wt.% FA was selected to produce the foams, to which varying quantities of carbonates were incorporated [2].

The processing temperature for compositions containing carbonate was set between 750 and 950 °C. This range is well above the dilatometric softening point of glass (590 °C), ensuring the necessary low viscosity for effective foaming. Additionally, this temperature interval aligns with the decomposition temperatures of the selected foaming agents. It was found that the density decreased with an increasing sintering temperature, reaching minimum values within the temperature range of around 850–900 °C; however, further increasing the heat treatment temperature to 950 °C caused an increase in the apparent density. Figure 10 illustrates the standard appearance of the glass foams post-rectifying.

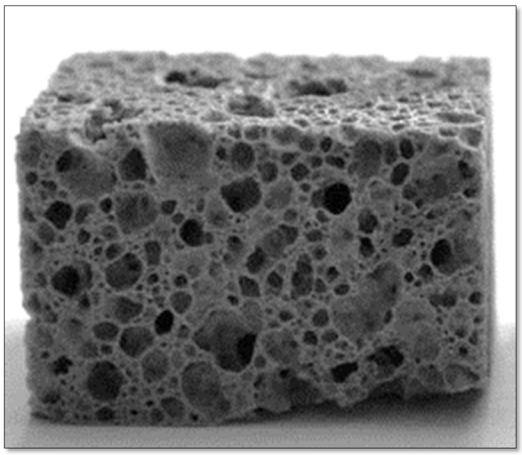


Figure 10. The typical aspect of the glass–ceramic composites after rectifying (adapted with permission from [2], Elsevier, 2009).

The study revealed that it is possible to achieve homogenous microstructures characterized by large pores by incorporating 1–2 wt.% carbonates and employing a low sintering temperature (850 °C). This process results in the production of foams with an apparent density and compressive strength in the ranges of approximately 0.36–0.41 g·cm^{-3} and 2.40–2.80 MPa, respectively. A strong correlation was found between the compressive strength, apparent density, and microstructural features such as pore size, strut thickness, and internal porosity. Furthermore, the crystalline phases within the glass foams evolved with increasing temperature; for example, compositions GAC1 and GAD1 exhibited the presence of quartz (ICDD card 46-1045) and tridymite (ICDD card 42-1401) at 750 °C, whereas the pyroxene phase augite, with the composition Ca(Mg,Fe,Al)(Si,Al)$_2$O$_6$ (ICDD card 00-41-1483), was observed to crystallize at 800 °C.

In general, glass foams depend on a similarly delicate balance between viscous flow sintering and gas evolution that is governed by many factors such as the nature and particle size of raw materials, firing temperatures and heating rate, gas atmosphere in a furnace, etc. Crystallization may occur as well, affecting the final physical, mechanical, and thermal properties of foam, namely density, compressive strength, thermal conductivity, and diffusivity [30]. To avoid excessive crystallization and to control both foaming and crystallization, the waste glasses with a limited tendency towards crystallization are used as the most suited starting material. In turn, the crystallization may be intentionally stimulated by using glass cullet mixed with foaming agents as well as with substances more prone to devitrification. Although substantial crystallization is negative for the development of highly porous foams, its advantage is the formation of an open-cell morphology of a three-dimensional trabecular structure.

Special attention must be given to choosing foaming additives. Although SiC may be quite expensive and have a negative impact on the overall cost/benefit balance, SiC could derive from the waste originated by the polishing of glass or traditional ceramics. Likewise, carbonaceous residues, as foaming agents, may derive from common industrial wastes [2,30,63]. Importantly, the foaming reaction must take place in a pyroplastic mass,

determined by the softening of glass powders, with a specified viscosity (in the order of 10^3–10^5 Pa·s [64]).

Another important issue to be considered is the particle size of FA. Thus, the influence of particle size on the sinterability and properties of sintered glass–ceramics has been discussed elsewhere [65]. Coal fly ash was separated into three size fractions, namely CFA, 20CFA, and 40CFA, with the median particle size (d50) of the powder being 12.6 μm, 7.5 μm, and 4.9 μm for CFA, 20CFA, and 40CFA, respectively. The sintering of the smaller particles was easier than for the larger ones, since the sintering activation energy of CFA was higher than 20CFA and 40CFA. However, regardless of particle size, the flexural strength of sintered glass–ceramics increased with a rise in temperature. The porosity and water absorption of the sintered samples gradually decreased when increasing the sintering temperature. Noticeably, with the finer the coal fly ash particles, a better sintering effect and better performance of the sintered glass–ceramics was achieved [65]. Likewise, it was demonstrated [66] that when the particle size of FA decreased, the linear shrinkage, bulk density, compressive strength, acid resistance, and thermal conductivity of lightweight insulation materials increased, but the apparent porosity decreased.

5. Conclusions

In the global scenario, the disposal of enormous amounts of FA is a major matter of concern because it represents a significant negative environmental impact, including the leaching of potentially toxic substances into soils and groundwater. Over the years, there has been an increasing interest in the use of FA for a variety of applications, since the reutilization of waste materials into novel high-added-value products is widely recognized as a challenge of high technologic interest. Likewise, encouraging results have been demonstrated in the preparation of both monolithic and cellular ceramics utilizing fly ash and other waste materials. In particular, the results discussed in this brief review demonstrate that FA can be successfully recycled into both bulk-nucleated glass–ceramics and porous glass–ceramic composites through the simultaneous control of both the formulations and manufacturing processes.

The composition of FA significantly depends on the coal type and technological processes used in thermal power plants. Vitrification is undoubtedly easier for wastes rich in glass-forming oxides, considering the fact that suitable glass-based products can be obtained only when an appropriate ratio between the glass network former and modifiers is attained.

Vitrification of a glass batch composed of merely coal FA was found to be difficult, or almost impossible. To produce glass–ceramic, the glass composition containing FA has to be modified through the addition of other ingredients in the form of natural raw materials, selected oxides, industrial wastes, etc. A key feature of FA-containing glasses is the availability of nucleating agents from the waste stream such as Fe_2O_3, SO_3, TiO_2, and P_2O_5. However, nucleating agents such as CaF_2, TiO_2, and Cr_2O_3 are intentionally added to the formulation of certain base glasses containing FA to promote controlled internal crystallization with the formation of desired crystalline phases resulting in dense glass–ceramics with high mechanical properties. Indeed, bulk-nucleated glass–ceramics demonstrate superior mechanical properties compared to sinter-crystallized glass—ceramics of the same compositions or to glass–ceramics without a preliminary vitrification step, i.e., direct sintering of wastes, especially if combined with recycled glasses.

Porous glass–ceramic composites are mainly produced by the powder method when a mixture of glass powders and pore-forming agents facilitating the formation of a gaseous phase is sintered upon heating. Thus, glass-based foams represent a further variant of glass sintering and depend on a delicate balance between viscous flow sintering and gas evolution. New technologies have been developed such as replica, sacrificial template, and direct foaming methods and the most straightforward and widely used way is direct foaming, namely, sintering a mixture of raw materials and a small number of additives. The type and content of foaming agents, along with the sintering temperature, affect

the resulting foam glass's apparent density, compressive strength, microstructure, and crystalline phase composition. The driving force in the sintering process is the surface energy of the powder, which is closely related to the particle size of the powder. Therefore, the introduction of different particle size of fly ash has a great influence on the properties of porous ceramic materials.

There are still many problems associated with high-temperature processing of bulk-nucleated glass–ceramics that should be taken into account upon designing new formulations containing FA.

Another open issue is the necessity to provide samples' toxicity characteristics, considering the presence of potentially toxic substances in FA not accommodated in the crystalline structures and remaining in glassy phase.

New technologies including additive manufacturing will be potentially useful in the transition from results obtained from laboratory trials to the industrial scale when dealing with the utilization of FA in glass-based materials.

Author Contributions: Conceptualization, H.R.F. and D.U.T.; methodology, H.R.F. and D.U.T.; validation, H.R.F., O.G. and D.U.T.; data curation, H.R.F., O.G. and D.U.T.; writing—original draft preparation, H.R.F., O.G. and D.U.T.; writing—review and editing, H.R.F., O.G. and D.U.T.; supervision, H.R.F. and D.U.T. All authors have read and agreed to the published version of the manuscript.

Funding: H.R.F. thanks the CICECO-Aveiro Institute of Materials, UIDB/50011/2020, UIDP/50011/2020, and LA/P/0006/2020 (through the FCT/MCTES (PIDDAC)).

Conflicts of Interest: The authors declare no conflicts of interest.

References

1. Nadaf, M.B.; Dutta, S.; Mandal, J.N. Fly Ash as Backfill Material in Slopes Using Waste PET Bottles as Reinforcement. In *Waste Management and Resource Efficiency*; Ghosh, S., Ed.; Springer: Singapore, 2019; pp. 905–913. [CrossRef]
2. Fernandes, H.R.; Tulyaganov, D.U.; Ferreira, J.M.F. Preparation and characterization of foams from sheet glass and fly ash using carbonates as foaming agents. *Ceram. Int.* **2009**, *35*, 229–235. [CrossRef]
3. Panias, D.; Giannopoulou, I.P.; Perraki, T. Effect of synthesis parameters on the mechanical properties of fly ash-based geopolymers. *Colloids Surf. A Physicochem. Eng. Asp.* **2007**, *301*, 246–254. [CrossRef]
4. Das, D.; Rout, P.K. Synthesis, Characterization and Properties of Fly Ash Based Geopolymer Materials. *J. Mater. Eng. Perform.* **2021**, *30*, 3213–3231. [CrossRef]
5. Roy, R.; Das, D.; Rout, P.K. Mullite Ceramics Derived from Fly Ash Powder by Using Albumin as an Organic Gelling Agent. *Biointerface Res. Appl. Chem.* **2023**, *13*, 339. [CrossRef]
6. Whiteside, M.; Herndon, J. Aerosolized Coal Fly Ash: Risk Factor for COPD and Respiratory Disease. *J. Adv. Med. Med. Res.* **2018**, *26*, 1–13. [CrossRef]
7. Yu, X.; Cui, Y.; Chen, Y.; Chang, I.S.; Wu, J. The drivers of collaborative innovation of the comprehensive utilization technologies of coal fly ash in China: A network analysis. *Environ. Sci. Pollut. Res.* **2022**, *29*, 56291–56308. [CrossRef]
8. Abbass, W.; Abbas, S.; Aslam, F.; Ahmed, A.; Ahmed, T.; Hashir, A.; Mamdouh, A. Manufacturing of Sustainable Untreated Coal Ash Masonry Units for Structural Applications. *Materials* **2022**, *15*, 4003. [CrossRef]
9. Daniel, C.W.; Tsang, L.W. (Eds.) *Low Carbon Stabilization and Solidification of Hazardous Wastes*, 1st ed.; Elsevier: Amsterdam, The Netherlands, 2021.
10. Koshlak, H. Synthesis of Zeolites from Coal Fly Ash Using Alkaline Fusion and Its Applications in Removing Heavy Metals. *Materials* **2023**, *16*, 4837. [CrossRef]
11. Gollakota, A.R.K.; Volli, V.; Shu, C.M. Progressive utilisation prospects of coal fly ash: A review. *Sci. Total Environ.* **2019**, *672*, 951–989. [CrossRef]
12. Jala, S.; Goyal, D. Fly ash as a soil ameliorant for improving crop production—A review. *Bioresour. Technol.* **2006**, *97*, 1136–1147. [CrossRef]
13. Ukwattage, N.L.; Ranjith, P.G.; Bouazza, M. The use of coal combustion fly ash as a soil amendment in agricultural lands (with comments on its potential to improve food security and sequester carbon). *Fuel* **2013**, *109*, 400–408. [CrossRef]
14. Das, D.; Rout, P.K. A Review of Coal Fly Ash Utilization to Save the Environment. *Water Air Soil Pollut.* **2023**, *234*, 128. [CrossRef]
15. Niraj, N.; Pandey, K.M.; Dey, A. Tribological behaviour of Magnesium Metal Matrix Composites reinforced with fly ash cenosphere. *Mater. Today Proc.* **2018**, *5*, 20138–20144. [CrossRef]
16. Wesche, K. *Fly Ash in Concrete—Properties and Performance*; CRC Press: London, UK, 1991.
17. Feng, S.; Li, Y. Study on coal fly ash classified by bulk density. *J. Phys. Conf. Ser.* **2021**, *1732*, 012127. [CrossRef]
18. Radenović, A. Inorganic constituents in coal. *Kem. Ind. Chem. Chem. Eng.* **2006**, *55*, 65–71.

19. Vassilev, S.V.; Vassileva, C.G. Methods for Characterization of Composition of Fly Ashes from Coal-Fired Power Stations: A Critical Overview. *Energy Fuels* **2005**, *19*, 1084–1098. [CrossRef]
20. Vassilev, S.V.; Vassileva, C.G. A new approach for the classification of coal fly ashes based on their origin, composition, properties, and behaviour. *Fuel* **2007**, *86*, 1490–1512. [CrossRef]
21. Vassilev, S.V.; Vassileva, C.G. Mineralogy of combustion wastes from coal-fired power stations. *Fuel Process. Technol.* **1996**, *47*, 261–280. [CrossRef]
22. Blissett, R.S.; Rowson, N.A. A review of the multi-component utilisation of coal fly ash. *Fuel* **2012**, *97*, 1–23. [CrossRef]
23. Vichaphund, S.; Aht-Ong, D.; Sricharoenchaikul, V.; Atong, D. Characteristic of fly ash derived-zeolite and its catalytic performance for fast pyrolysis of Jatropha waste. *Environ. Technol. UK* **2014**, *35*, 2254–2261. [CrossRef]
24. Franus, W.; Wiatros-Motyka, M.M.; Wdowin, M. Coal fly ash as a resource for rare earth elements. *Environ. Sci. Pollut. Res.* **2015**, *22*, 9464–9474. [CrossRef] [PubMed]
25. *ASTM C618-12*; Standard Specification for Coal Fly Ash and Raw or Calcined Natural Pozzolan for Use in Concrete. American Society for Testing and Materials International: West Conshohocken, PA, USA, 2019. [CrossRef]
26. Hardjito, D.; Wallah, S.E.; Sumajouw, D.M.J.; Rangan, B.V. On the development of fly ash-based geopolymer concrete. *ACI Mater. J.* **2004**, *101*, 467–472. [CrossRef]
27. Xu, G.; Shi, X. Characteristics and applications of fly ash as a sustainable construction material: A state-of-the-art review. *Resour. Conserv. Recycl.* **2018**, *136*, 95–109. [CrossRef]
28. Ciećko, Z.; Żołnowski, A.C.; Madej, M.; Wasiak, G.; Lisowski, J. Long-Term effects of hard coal fly ash on selected soil properties. *Pol. J. Environ. Stud.* **2015**, *24*, 1949–1957. [CrossRef] [PubMed]
29. Rawlings, R.D.; Wu, J.P.; Boccaccini, A.R. Glass-ceramics: Their production from wastes—A Review. *J. Mater. Sci.* **2006**, *41*, 733–761. [CrossRef]
30. Rincón, A.; Marangoni, M.; Cetin, S.; Bernardo, E. Recycling of inorganic waste in monolithic and cellular glass-based materials for structural and functional applications. *J. Chem. Technol. Biotechnol.* **2016**, *91*, 1946–1961. [CrossRef] [PubMed]
31. Vu, D.H.; Wang, K.S.; Chen, J.H.; Nam, B.X.; Bac, B.H. Glass-ceramic from mixtures of bottom ash and fly ash. *Waste Manag.* **2012**, *32*, 2306–2314. [CrossRef] [PubMed]
32. Erol, M.; Genç, A.; Öveçoğlu, M.L.; Yücelen, E.; Küçükbayrak, S.; Taptik, Y. Characterization of a glass-ceramic produced from thermal power plant fly ashes. *J. Eur. Ceram. Soc.* **2000**, *20*, 2209–2214. [CrossRef]
33. Kim, J.M.; Kim, H.S. Processing and properties of a glass-ceramic from coal fly ash from a thermal power plant through an economic process. *J. Eur. Ceram. Soc.* **2004**, *24*, 2825–2833. [CrossRef]
34. Barbieri, L.; Lancellotti, I.; Manfredini, T.; Queralt, I.; Rincon, J.M.; Romero, M. Design, obtainment and properties of glasses and glass-ceramics from coal fly ash. *Fuel* **1999**, *78*, 271–276. [CrossRef]
35. Waraporn, E.; Shigeki, M. Preparation of Glass-Ceramics Using Fly Ash as a Raw Material. *J. Sci. Technol.* **2005**, *13*, 137–142.
36. Shang, W.; Peng, Z.; Xu, F.; Tang, H.; Rao, M.; Li, G.; Jiang, T. Preparation of enstatite-spinel based glass-ceramics by co-utilization of ferronickel slag and coal fly ash. *Ceram. Int.* **2021**, *47*, 29400–29409. [CrossRef]
37. Yu, J.; Peng, Z.; Shang, W.; Chen, Q.; Zhu, G.; Tang, H.; Rao, M.; Li, G. Dual roles of Cr_2O_3 in preparation of glass-ceramics from ferronickel slag. *Ceram. Int.* **2023**, *49*, 15947–15958. [CrossRef]
38. Karamanov, A.; Pelino, M. Evaluation of the degree of crystallisation in glass-ceramics by density measurements. *J. Eur. Ceram. Soc.* **1999**, *19*, 649–654. [CrossRef]
39. Alizadeh, P.; Marghussian, V.K. The effect of compositional changes on the crystallization behaviour and mechanical properties of diopside-wollastonite glass-ceramics in the SiO_2-CaO-MgO (Na_2O) system. *J. Eur. Ceram. Soc.* **2000**, *20*, 765–773. [CrossRef]
40. Karamanov, A.; Taglieri, G.; Pelino, M. Iron-rich sintered glass-ceramics from industrial wastes. *J. Am. Ceram. Soc.* **1999**, *82*, 3012–3016. [CrossRef]
41. Vasilopoulos, K.C.; Tulyaganov, D.U.; Agathopoulos, S.; Karakassides, M.A.; Ferreira, J.M.F.; Tsipas, D. Bulk nucleated fine grained mono-mineral glass-ceramics from low-silica fly ash. *Ceram. Int.* **2009**, *35*, 555–558. [CrossRef]
42. Vasilopoulos, K.C.; Tulyaganov, D.U.; Agathopoulos, S.; Karakassides, M.A.; Ribeiro, M.; Ferreira, J.M.F.; Tsipas, D. Vitrification of low silica fly ash: Suitability of resulting glass ceramics for architectural or electrical insulator applications. *Adv. Appl. Ceram.* **2009**, *108*, 27–32. [CrossRef]
43. Tulyaganov, D.U.; Dimitriadis, K.; Agathopoulos, S.; Baino, F.; Fernandes, H.R. Wollastonite-containing glass-ceramics from the CaO–Al_2O_3–SiO_2 and CaO–MgO–SiO_2 ternary systems. *Open Ceram.* **2024**, *17*, 100507. [CrossRef]
44. Tulyaganov, D.U.; Dimitriadis, K.; Agathopoulos, S.; Fernandes, H.R. Glasses and glass-ceramics in the CaO–MgO–SiO_2 system: Diopside containing compositions—A brief review. *J. Non. Cryst. Solids* **2023**, *612*, 122351. [CrossRef]
45. Koukouzas, N.K.; Zeng, R.; Perdikatsis, V.; Xu, W.; Kakaras, E.K. Mineralogy and geochemistry of Greek and Chinese coal fly ash. *Fuel* **2006**, *85*, 2301–2309. [CrossRef]
46. Gitzen, W.H. *Alumina as a Ceramic Material*; American Ceramic Society: Columbus, OH, USA, 2006; ISBN 978-0-916094-46-1.
47. Tulyaganov, D.U.; Tukhtaev, M.E.; Escalante, J.I.; Ribeiro, M.J.; Labrincha, J.A. Processing of cordierite based ceramics from alkaline-earth-aluminosilicate glass, kaolin, alumina and magnesite. *J. Eur. Ceram. Soc.* **2002**, *22*, 1775–1782. [CrossRef]
48. Ganatsios, S.; Maropoulos, S.; Papanikolaou, S.; Gheorghe, G.; Dontu, O.; Seritan, G.; Besnea, D. Novel bulk and porous glass ceramics produced by waste materials. *Rom. Rev. Precis. Mech. Opt. Mechatron.* **2015**, *48*, 186–189.

49. Ganatsios, S.; Maropoulos, S.; Papanikolaou, S.; Dontu, O.; Besnea, D.; Spânu, A.; Gheorghe, G.I. Sustainability of waste material reutilization into novel glass ceramics: A life cycle analysis. *Rom. Rev. Precis. Mech. Opt. Mechatron.* **2016**, *50*, 53–56.
50. Dimitriadis, K.; Moschovas, D.; Tulyaganov, D.U.; Agathopoulos, S. Development of novel bioactive glass-ceramics in the Na_2O/K_2O-CaO-MgO-SiO_2-P_2O_5-CaF_2 system. *J. Non-Cryst. Solids* **2020**, *533*, 119936. [CrossRef]
51. Kaur, G.; Kumar, V.; Baino, F.; Mauro, J.C.; Pickrell, G.; Evans, I.; Bretcanu, O. Mechanical properties of bioactive glasses, ceramics, glass-ceramics and composites: State-of-the-art review and future challenges. *Mater. Sci. Eng. C* **2019**, *104*, 109895. [CrossRef] [PubMed]
52. Wang, M.; Xu, S. Preparation and Applications of Foam Ceramics. *IOP Conf. Ser. Earth Environ. Sci.* **2018**, *186*, 012066. [CrossRef]
53. Yu, G.; Gao, W.; Yao, Y.; Zhang, T.; Fu, Y.; Kong, X. Recycling of Silicomanganese Slag and Fly Ash for Preparation of Environment-Friendly Foamed Ceramics. *Materials* **2023**, *16*, 6724. [CrossRef] [PubMed]
54. Cao, W.; Cheng, X.; Gong, L.; Li, Y.; Zhang, R.; Zhang, H. Thermal conductivity of highly porous ceramic foams with different agar concentrations. *Mater. Lett.* **2015**, *139*, 66–69. [CrossRef]
55. Zhu, L.; Li, S.; Li, Y.; Xu, N. Novel applications of waste ceramics on the fabrication of foamed materials for exterior building walls insulation. *Constr. Build. Mater.* **2018**, *180*, 291–297. [CrossRef]
56. Zhou, L.Z.; Wang, C.A.; Huang, Y. Effects of the Starting Powders on Microstructure and Properties of Porous Silica Ceramics. *Key Eng. Mater.* **2010**, *434–435*, 674–677.
57. Chen, T.; Peng, T.; Sun, H.; Li, X.; Xiao, S.; You, D.; Chu, L.; Wu, M.; Zhang, T.; Tang, Y.; et al. Diopside-like based ceramics prepared via one-step sintering of extracted titanium slag and coal fly ash. *Ceram. Int.* **2024**, *50*, 14040–14053. [CrossRef]
58. Wang, S.; Li, X.; Zou, B.; Ma, Z.; Yu, W. Design and performance of lightweight high–temperature resistant microwave penetrating foamed ceramics. *Ceram. Int.* **2024**, *50*, 13974–13981. [CrossRef]
59. Dong, X.; Han, F.; Yu, N.; Li, M. Preparation and characterization of novel spontaneous foam ceramics based on all-solid waste. *J. Alloys Compd.* **2024**, *976*, 173135. [CrossRef]
60. Zhu, M.; Ji, R.; Li, Z.; Wang, H.; Liu, L.L.; Zhang, Z. Preparation of glass ceramic foams for thermal insulation applications from coal fly ash and waste glass. *Constr. Build. Mater.* **2016**, *112*, 398–405. [CrossRef]
61. Bai, J.; Yang, X.; Xu, S.; Jing, W.; Yang, J. Preparation of foam glass from waste glass and fly ash. *Mater. Lett.* **2014**, *136*, 52–54. [CrossRef]
62. Zhang, R.; Feng, J.; Cheng, X.; Gong, L.; Li, Y.; Zhang, H. Porous thermal insulation materials derived from fly ash using a foaming and slip casting method. *Energy Build.* **2014**, *81*, 262–267. [CrossRef]
63. Ding, L.; Ning, W.; Wang, Q.; Shi, D.; Luo, L. Preparation and characterization of glass-ceramic foams from blast furnace slag and waste glass. *Mater. Lett.* **2015**, *141*, 327–329. [CrossRef]
64. Sarkar, T.; Naskar, M.K.; Chakraborty, A.; Roy, P.K.; Chakraborty, S. Preparation of high-strength waste-derived eco-friendly ceramic foam as face brick and its estimation of building energy consumption for thermal insulation. *J. Build. Eng.* **2024**, *88*, 109043. [CrossRef]
65. Zeng, L.; Sun, H.-J.; Peng, T.-J.; Zheng, W.-M. The sintering kinetics and properties of sintered glass-ceramics from coal fly ash of different particle size. *Results Phys.* **2019**, *15*, 102774. [CrossRef]
66. Chen, R.; Li, Y.; Xiang, R.; Li, S. Effect of particle size of fly ash on the properties of lightweight insulation materials. *Constr. Build. Mater.* **2016**, *123*, 120–126. [CrossRef]

Disclaimer/Publisher's Note: The statements, opinions and data contained in all publications are solely those of the individual author(s) and contributor(s) and not of MDPI and/or the editor(s). MDPI and/or the editor(s) disclaim responsibility for any injury to people or property resulting from any ideas, methods, instructions or products referred to in the content.